JOURNAL OF MATERIALS SCIENCE 18 (1983) 827–839

A new approach to the theory of grain boundaries

M. J. MARCINKOWSKI
Department of Mechanical Engineering and Engineering Materials Group, University of Maryland, College Park, Maryland 20742, USA

It is shown that the classical picture of a grain boundary in terms of a single array of lattice dislocations is incomplete. In addition, it is also necessary to incorporate into the boundary a second array of continuously distributed surface dislocations of infinitesimal strength and of opposite sign to those of the lattice dislocations, but with the same total magnitude. Furthermore, the lattice dislocations can also dissociate into a continuous distribution by the formation of cores. As the angular misorientation of the grain boundary increases, more and more of the surface dislocations combine with the lattice dislocations, in turn resulting in the formation of a larger and larger stress-free ledge, with a consequent overall reduction in the strength of the remaining lattice dislocation.

1. Introduction

In 1953 the first dramatic proof was given for the existence of crystal lattice dislocations when Vogel, Pfann, Corey and Thomas [1] showed that the misorientation angle θ associated with a low-angle symmetric tilt boundary in germanium, as measured by X-rays, correlated with the spacing between etch pits h in the boundary according to the theoretically predicted relation

$$\mathbf{b}_L = h\theta \qquad (1)$$

where $\mathbf{b}_L$ is the Burger's vector of the crystal lattice dislocation. This initial finding led to a burst of activity in the study of grain boundaries, the results of which have been extensively described in a number of places [2–4]. Surprisingly, however, when the simple concept embodied in Equation 1 was applied to grain boundaries of arbitrarily large angular misorientation, the results were not so straightforward. It was argued that the difficulty might perhaps be due to the small value of h in Equation 1 for large angles which caused the dislocation cores to overlap. This argument, however, implied that the basic theory was still sound and that it was simply a technical problem to somehow account for the properties, i.e. distortions, energy, etc. of a more or less conventional dislocation core. So much attention was placed on this one aspect of the problem that the question of whether or not the basic theory of grain boundaries itself might in fact contain some basic conceptual errors was left unanswered. It is instructive to consider in some detail how these errors could be allowed to creep into one of the cornerstones of dislocation theory and become sufficiently entrenched within it so as to retard progress in the understanding of surfaces and interfaces in general, wherein grain boundaries play only a part. In what follows, it will be shown that a number of very important fundamental concepts associated with dislocation theory are embodied in the low-angle grain boundary relationship given by Equation 1. They are the concepts of (a) an image dislocation, (b) a dislocation core, (c) quantization of a dislocation and (d) a wall of dislocations. These will now be considered in some detail.

2. The individual crystal lattice dislocation

Consider the single edge dislocation in Fig. 1a contained within a finite solid. It is represented by the terminus of an extra half plane which is squeezed to a point. This dislocation gives rise to stresses on the surface of the finite body. These stresses can be removed by the introduction of image dislocations as first proposed by Head [4]

0022–2461/83/030827–13$04.06/0

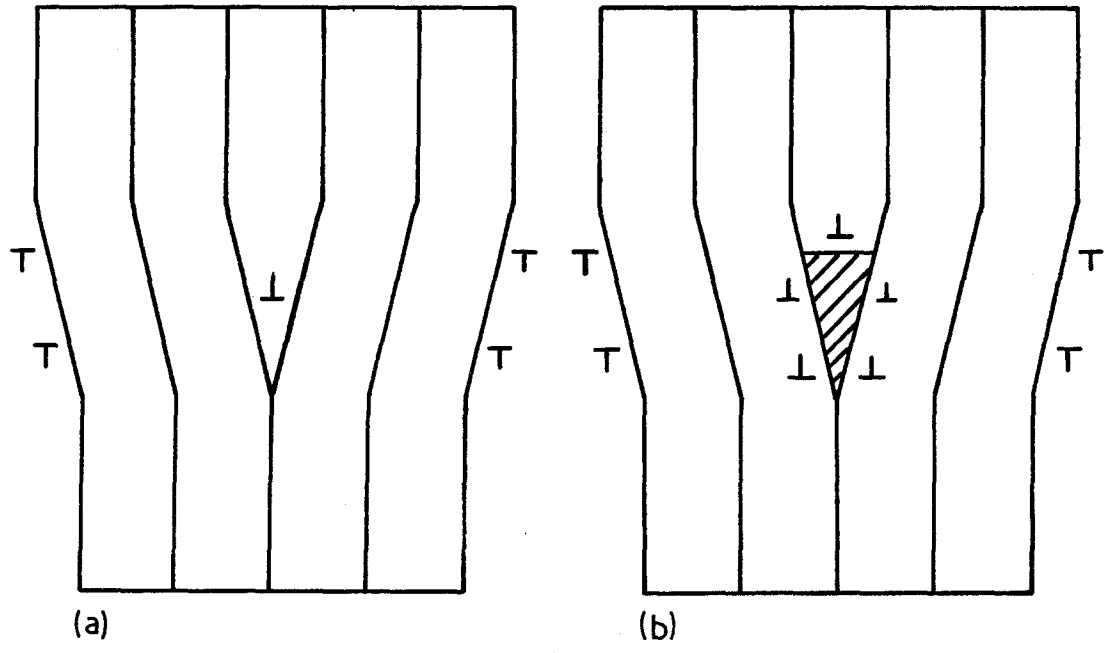

Figure 1 (a) Undissociated (b) dissociated edge dislocation, along with its corresponding surface dislocations.

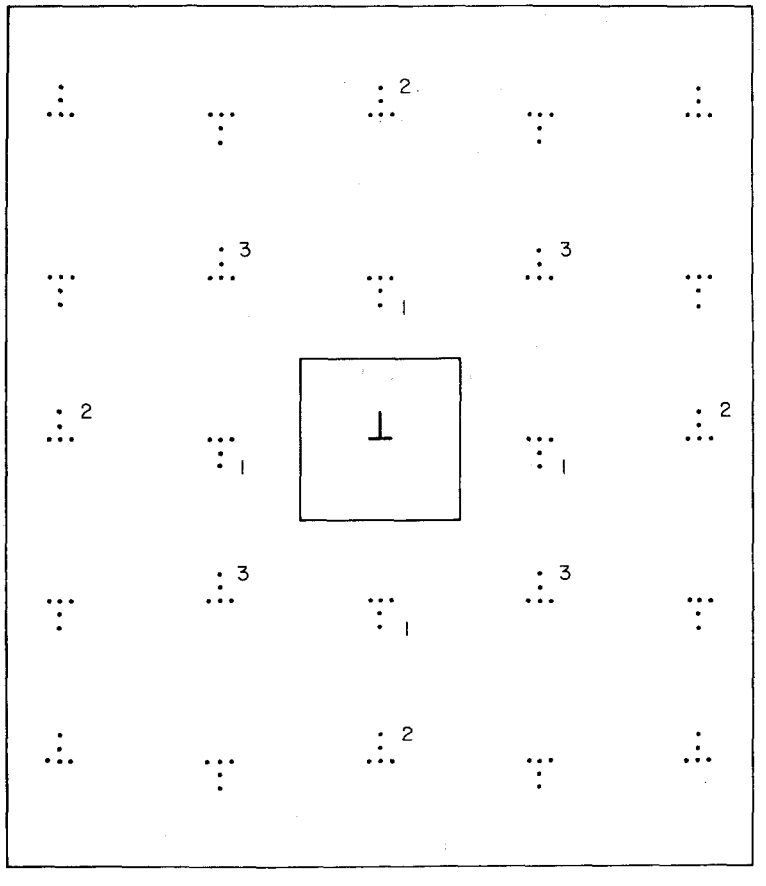

Figure 2 Image dislocation model used to insure that the stresses vanish on the surface of a finite body containing a dislocation.

in 1953. In the present case, this would involve the introduction of an infinite array of such dislocations, a portion of which are shown dotted in Fig. 2. The dislocations labelled with 1 are primary images. Those labelled with 2 are secondary images which are in fact images of the primary images from parallel faces. The images labelled with 3 are images of the primary images but arising from a surface at right angles to that which produced the primary image and so forth. Clearly, this is an extremely cumbersome approach, both from a mathematical as well as from a physical perspective, and can lead to great confusion. In fact, this image dislocation approach actually hinders a clear understanding of the grain boundary problem, as will be shortly demonstrated.

The most straightforward method of removing the surface tractions associated with the dislocation in Fig. 1a is to introduce a continuous distribution of infinitesimal dislocations on the surface of the body, the so called surface dislocation [5, 6] in the manner shown. The surface dislocations obey the following simple but powerful conservation law:

$$\mathbf{b}_L + \Sigma \mathbf{b}_S = 0 \qquad (2)$$

where $\mathbf{b}_L$ is the Burger's vector of the lattice dislocation, while $\mathbf{b}_S$ is that of the surface dislocation. For clarity $\mathbf{b}_S$ is chosen as $-\mathbf{b}_L/4$ in Fig. 1a, so that there are only four surface dislocations, all of opposite sign to that of the lattice dislocation. The distribution of the surface dislocations can be readily determined using well known numerical or integral equation techniques [7, 8]. Also important to note is that the distribution of surface dislocations is directly related to the shape or distortion of the external surface of the body, a point not at all obvious from the image dislocation model. This particular consideration is of paramount significance in the correct understanding of the grain boundary problem.

Since the extra half plane associated with the edge dislocation of Fig. 1a is shown with its terminus squeezed to a point, a singularity is generated at this point. It is the usual custom to imagine a hole to be drilled along the dislocation line in order to remove the singularity [9]. If this is done however, the physics of the problem becomes incorrect since it is not possible for this hole to glide along with the dislocation. A more realistic model would be to assume the formation of an asymmetric tensile crack just below the extra half plane such as depicted by the shaded area of Fig. 1b which may also be viewed as the dislocation core. In this figure the lattice dislocation, which was initially concentrated at a single point, is now allowed to dissociate into a continuous distribution of surface or crack dislocations [5]. Equilibrium is attained when the strain energy release occasioned by the dissociation is just balanced by the increase in surface energy due to crack formation. Needless to say, there are difficulties associated with a precise evaluation of the surface energy because of the small interplanar spacings, nevertheless the qualitative picture of the dissociation process remains correct. The surface dislocation arrays in Figs. 1a and b remain virtually unaltered by the core dissociation. Another important feature of Fig. 1b is that the dislocation core, unlike a simple hole, is highly structured in the form of an asymmetric tensile crack. Finally, Fig. 1b may be viewed as a doubly-connected body, all of whose surfaces are covered with a continuous distribution of surface dislocations arranged such that the surface tractions are reduced to zero.

3. Dislocation arrays which comprise grain boundaries

Consider next the stepped surface of Fig. 3a. Each step or ledge may be viewed as arising from the following reaction toward the right:

$$\mathbf{b}_L + \Sigma \mathbf{b}_S \rightleftharpoons L \qquad (3)$$

where L denotes the strength of the ledge. This reaction may also be viewed as the process wherein the surface dislocations completely annihilate with the crystal lattice dislocations with the resultant removal of their stress and strain fields. This is indicated by the dislocation pairs of opposite sign at each ledge in Fig. 3a.

Suppose now that the stepped surface in Fig. 3a is flattened into a planar configuration such as depicted in Fig. 3b, where the original undeformed positions of the body are shown as dashed lines. Such a process is formally equivalent to uncoupling the surface dislocations from the ledge and uniformly distributing them over the surfaces between the ledges [6]. In terms of Equation 3, this means the reaction toward the left. The lattice dislocations are similar to that shown in Fig. 1a in that they terminate at a point and thus possess no cores. An important difference however is that unlike the case in Fig. 1a, the inclined surface in Fig. 3b is not stress free. On

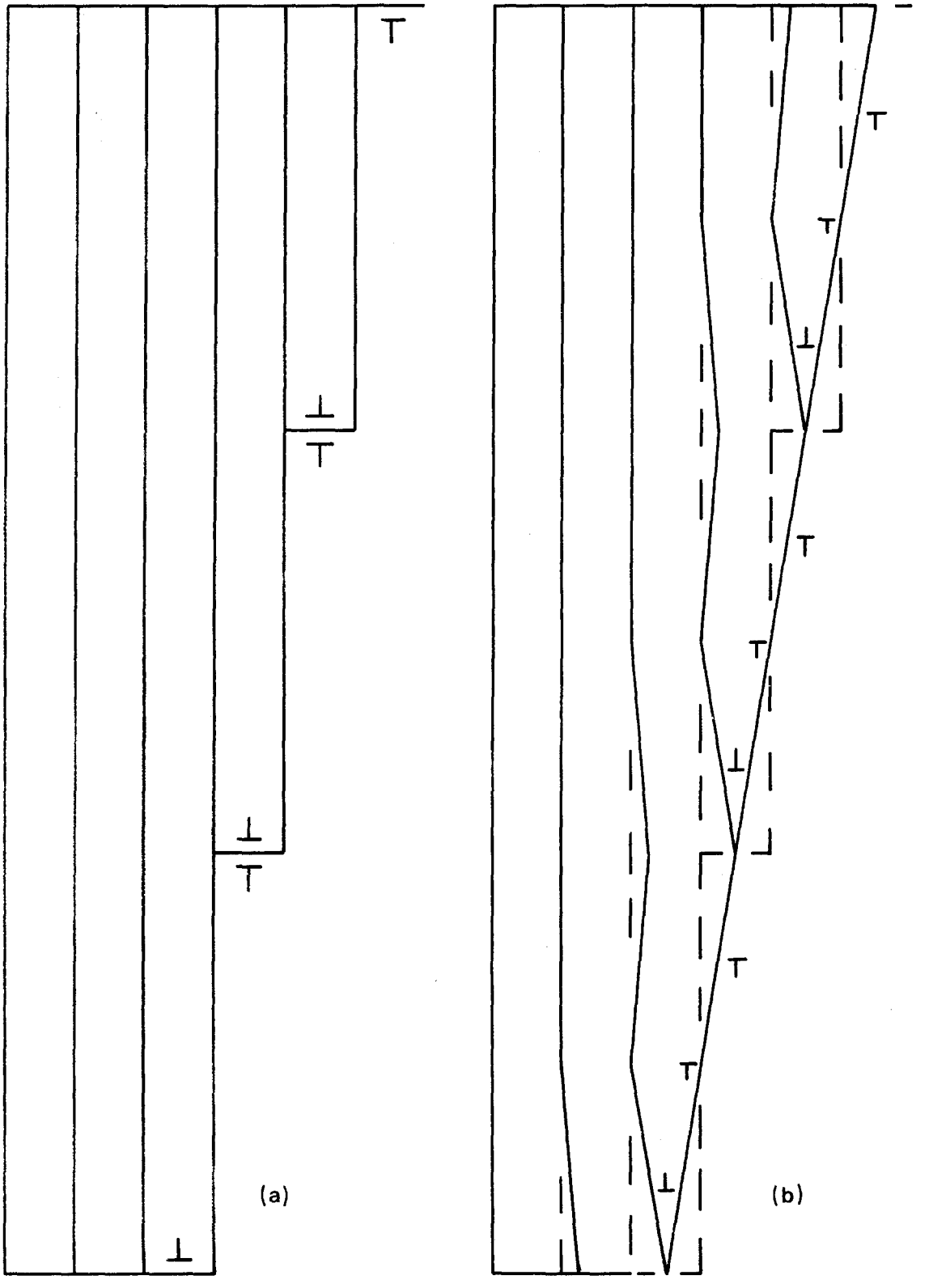

Figure 3 Stepped surface (a) before (b) after elastic deformation into a single plane.

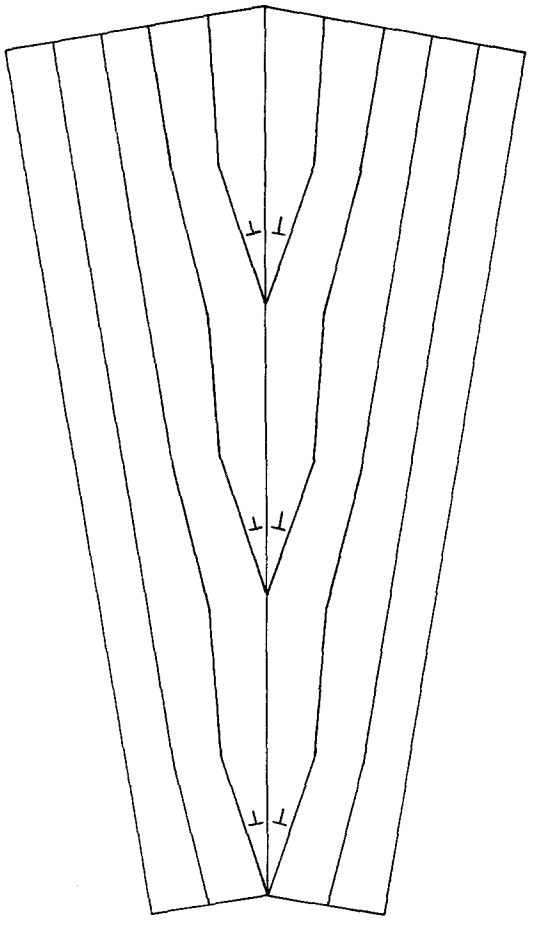

Figure 4 Creation of a symmetric tilt boundary by the joining of the body shown in Fig. 3b to its mirror image.

the other hand, the stresses that are present are only on the order of the spacing between lattice dislocations as will be shown shortly. This becomes clear when it is realized that the surface and lattice dislocations can be viewed as dipoles distributed along the surface of the crystal. Also important to realize in Fig. 3b is that the concept of an image dislocation breaks down completely, whereas no such problem is encountered with the surface dislocation concept.

If the body depicted in Fig. 3b is now joined to its mirror image, the symmetric tilt boundary of misorientation angle $\theta = 18.9$ shown in Fig. 4 obtains. For the purposes of clarity, the surface dislocations have been omitted from this figure. On the other hand, the dislocation configuration associated with this particular grain boundary can be portrayed somewhat more schematically as depicted in Fig. 5a. The large dislocation symbol represents that due to the lattice dislocation, while the small symbols denote the surface dislocations. It was originally thought [5, 10, 11] that the surface dislocations, in analogy with Fig. 1a, served as a screening array, as depicted in Fig. 5b. This model, however, was dropped in favour of that shown in Fig. 5a since the dislocations in the screening array were not confined to any well-defined surface and is thus a violation of one of the fundamental tenets of surface dislocation theory. The screening array did however obey the powerful conservation relation given by Equation 2. On the other hand, the classic description of a grain boundary does not even admit the existence of surface dislocations, but instead represents it in terms of an array of lattice dislocations as shown in Fig. 5c.

At first glance, it is rather astonishing that the surface dislocations within the grain boundary could have been completely overlooked. How could such a glaring omission have come about? The most likely explanation is as follows. First consider the shear stress field σ_{xy} at some point x, y arising from an infinite wall of edge dislocations spaced at a distance h from one another which can be written as [9]

$$\sigma_{xy} = \frac{\mu b_L}{2\pi(1-\nu)} \sum_{n=-\infty}^{+\infty} \frac{x[x^2-(y-nh)^2]}{[x^2+(y-nh)^2]^2} \tag{4}$$

and can be evaluated to give

$$\sigma_{xy} = \frac{\mu b_L}{2\pi(1-\nu)} \frac{\pi^2 x}{h^2} \frac{\left(\cosh\frac{2\pi x}{h}\right)\left(\cos\frac{2\pi y}{h}\right)-1}{2\left(\sinh^2\frac{\pi x}{h}+\sin^2\frac{\pi y}{h}\right)^2} \tag{5}$$

where it can be shown that the stresses practically vanished at distances from the grain boundary of the order of h. Because of this absence of long range stress, there seemed to be no reason to look for surface dislocations or their image dislocation analogue, if indeed one exists. Even more insidious is the fact that the surface dislocation array is continuous and uniform, and in the case of an infinite array, there is no stress field produced. This can be seen by rewriting the finite sum of Equation 4 in terms of a continuous distribution as follows [3]:

$$\sigma_{xy} = \frac{(\mu b_L/h)}{2\pi(1-\nu)} \int_{-L}^{+L} \frac{x[x^2-(y-y')^2]}{[x^2+(y-y')^2]^2} dy' \tag{6}$$

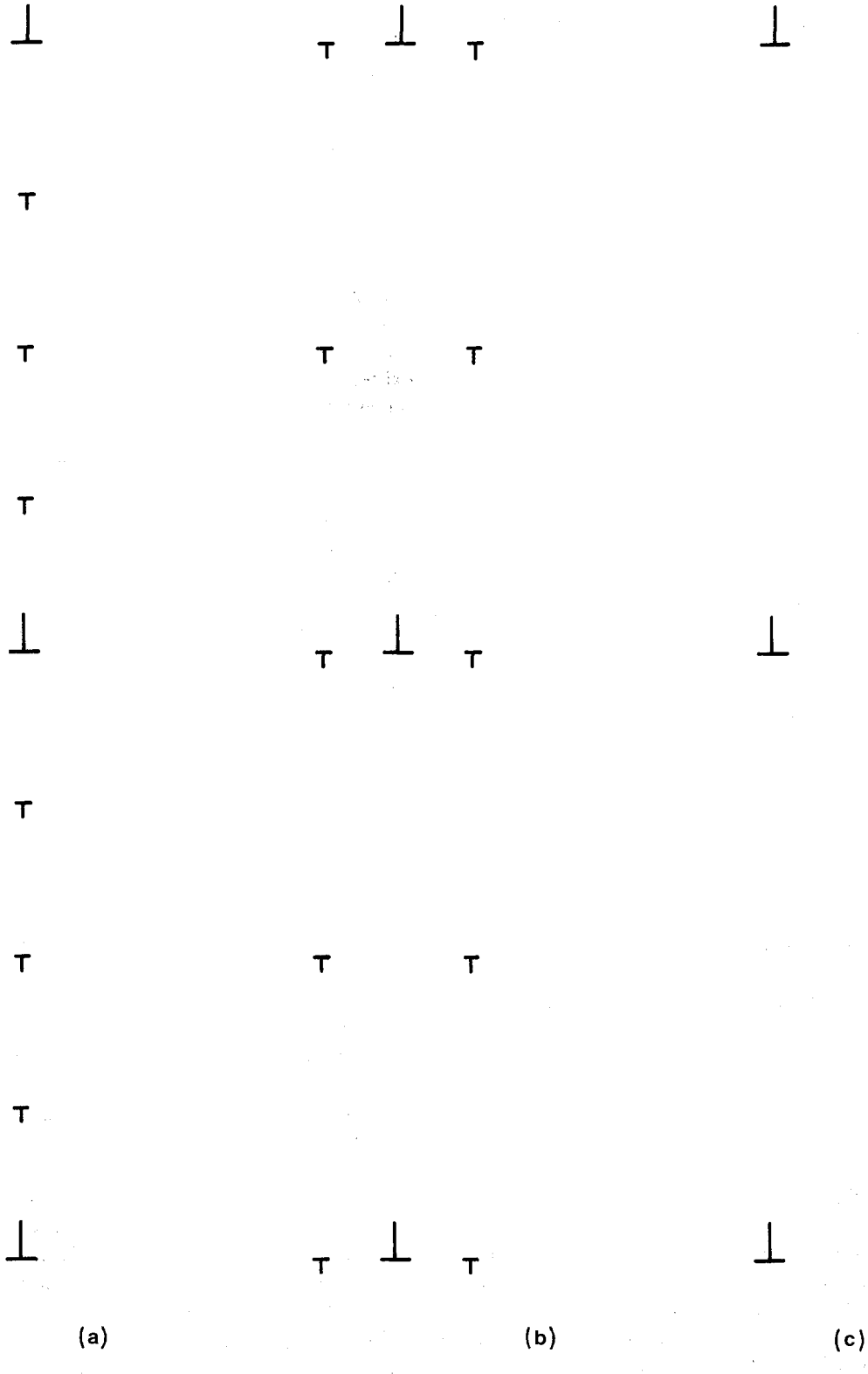

Figure 5 Grain boundary of Fig. 4 described in terms of (a) lattice and surface dislocations; (b) lattice and a screening dislocation array; (c) lattice dislocations only; (d) periodic unit removed from array in Fig. 5a; (e) and (f) correspond to dislocation arrays derived from the configurations shown in Figs. 6a and b, respectively.

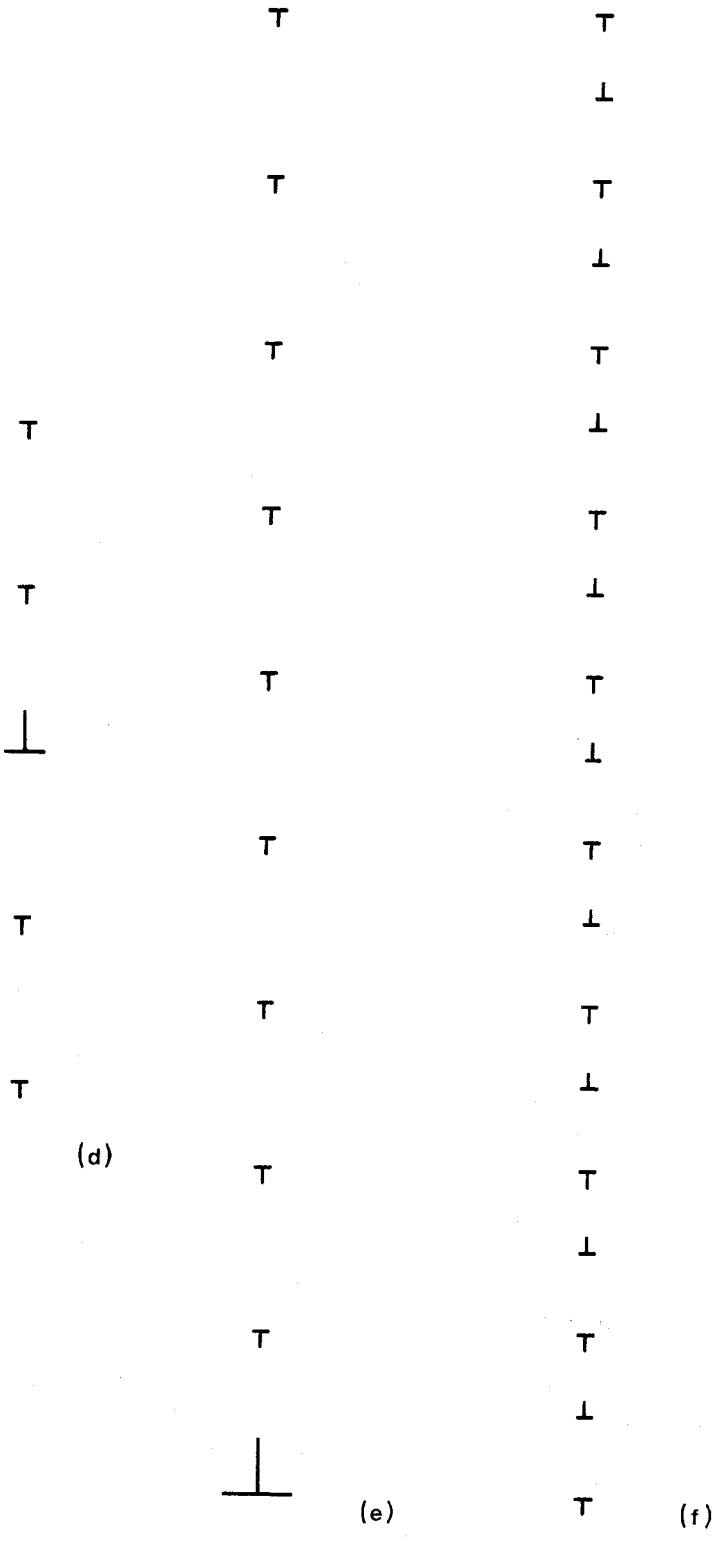

Figure 5 Continued.

where $2L$ is the length of the array. The integral can be evaluated to yield

$$\sigma_{xy} = \frac{(\mu b_L/h)}{2\pi(1-\nu)} \frac{2Lx(x^2-y^2+L^2)}{[x^2+(y+L)^2][x^2+(y-L)^2]} \quad (7)$$

where it is clear that as L goes to ∞, $\sigma_{xy} \to 0$. Another advantage of the surface dislocation array shown in Fig. 5a is that it allows one to consider only a unit of this boundary of length h such as shown in Fig. 5d for the purposes of various energy calculations, since the stress fields of all the other dislocations lying outside this distance are screened off from the unit under consideration. The screening array of Fig. 5b possesses this same advantage and has been utilized accordingly [11, 12]. On the other hand, the conventional model of a grain boundary depicted in Fig. 5c cannot be treated in this way since the short range stress field about such a boundary depends upon the interaction of any given dislocation with all of the others in the infinite array in the manner prescribed by Equation 4.

Since the classical description of a grain boundary such as given by Fig. 5c is incorrect, it seems only natural to inquire as to whether any physical meaning is to be attached to a single wall of dislocations of one sign. The answer to this question is best solved by reference to the drawing illustrated in Fig. 6a. Here the rightmost face of the body, whose initially undeformed position is drawn dashed has been elastically deformed into a flat inclined surface. Such a deformation is equivalent to uniform distribution of surface dislocations of one sign on the deformed surface. On the other hand, the creation of this array must also at the same time give rise to a single super dislocation of opposite sign at the bottom surface of the body in accordance with the conservation law of Equation 2. If the body in Fig. 6a is joined to its mirror image, the dislocation configuration of Fig. 5e obtains. It is to be emphasized that the configuration of Fig. 5e is not a grain boundary *per se* but is the limiting case of the grain boundary depicted in Fig. 5a as $h \to \infty$. Under these conditions, the super dislocation in Fig. 5e becomes infinite in strength.

There is yet another limiting case of the grain boundary shown in Fig. 5a. This occurs when the steps in Fig. 3a are made infinitesimal in length and distributed uniformly over the surface of the body in a manner such as approximated by Fig. 6b. If the surface is next flattened, similar to that illustrated in Fig. 3b, and joined to its mirror image, the configuration depicted in Fig. 7 is obtained, while the corresponding dislocation morphology is given in Fig. 5f. Here we see a uniform and continuous array of dipoles which represents the limiting case where $h \to 0$ and $b_L \to 0$. This limit also corresponds physically to a pair of smooth inclined surfaces associated with each grain that can be joined together to form a perfectly matched, i.e. no gaps or voids, stress-free grain boundary. On the other hand, such an arrangement cannot be realized in actual crystals because the ledge lengths are quantized by the crystal structure of the lattice which is in turn determined by the size of the atoms. Thus, the ledges cannot be subdivided infinitely, but are restricted in magnitude by the interatomic spacing of the crystal lattice so that all grain boundaries must be more or less of the type represented in Fig. 5a.

4. The unique behaviour of grain boundary dislocation cores

It follows that the grain boundary dislocation configuration of Fig. 4, in analogy with the single lattice dislocation of Fig. 1b, possesses a high elastic strain energy which can be lowered by the formation of asymmetric cracks or cores at the terminus of the extra half planes, similar to that illustrated in Fig. 1b. The resulting grain boundary configuration is depicted in Fig. 8 where the dislocation cores are again denoted by shaded areas. A new and important factor, which was not present for the isolated dislocation core of Fig. 1b now enters the picture for the grain boundary dislocation cores. This is the fact that the formation of the grain boundary cores involves the annihilation of a portion of the lattice dislocation, which is now distributed about the core, with an equal number of dislocations which were originally located within the area of the core before it was formed. For example, if the core length along the grain boundary is given by L_c then the strength of the lattice dislocation at the boundary is reduced by an amount given by $(L_c/h)\mathbf{b}_L$ where, as usual, h is the separation between the lattice dislocations in the boundary. The accompanying reduction in strength or compensation of the lattice dislocation by the surface dislocations takes place in accordance with Equation 3 to the right where an accompanying increment in ledge length ΔL is the

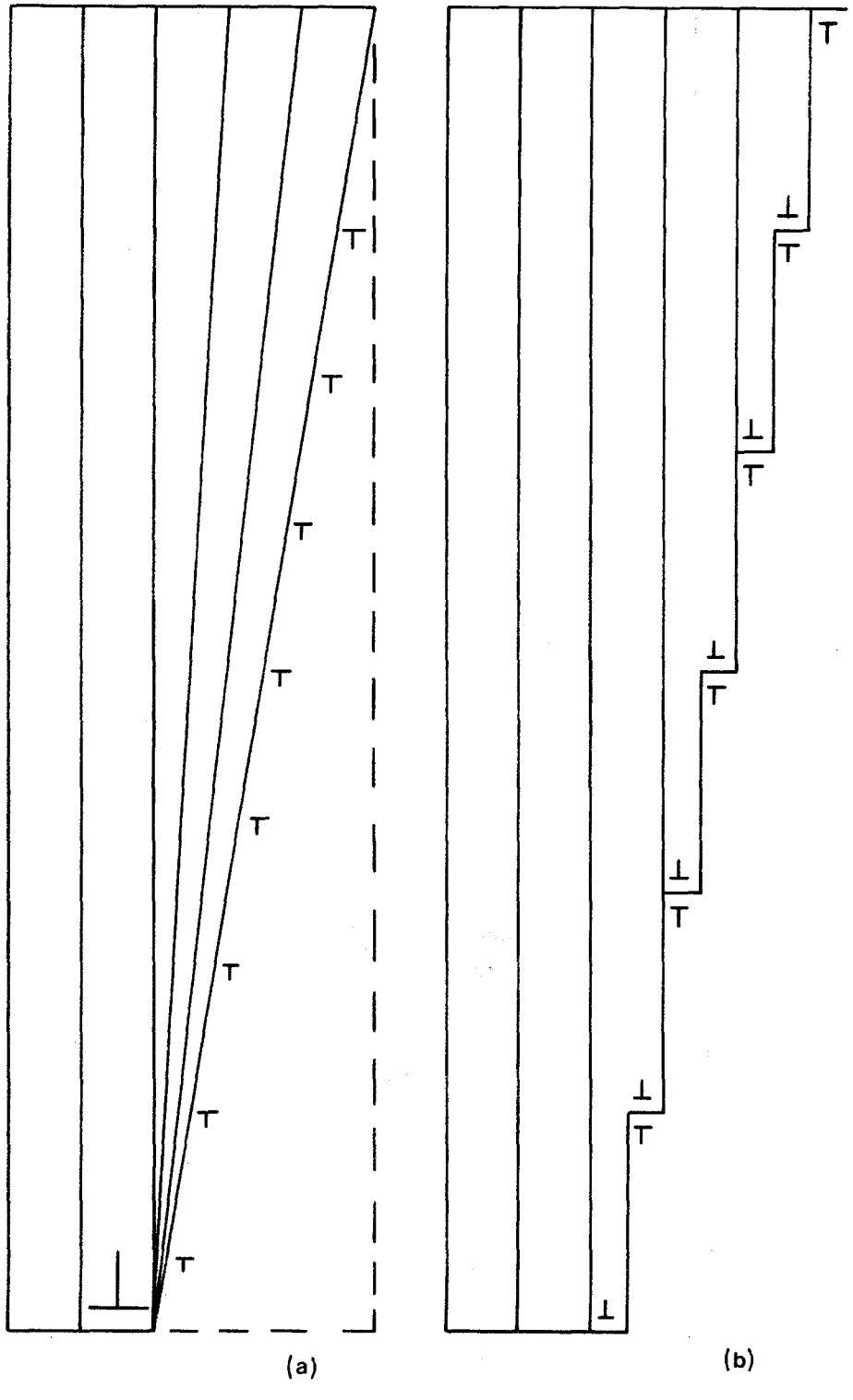

Figure 6 Creation of inclined surface by means of a uniform array of (a) surface dislocations (b) surface steps.

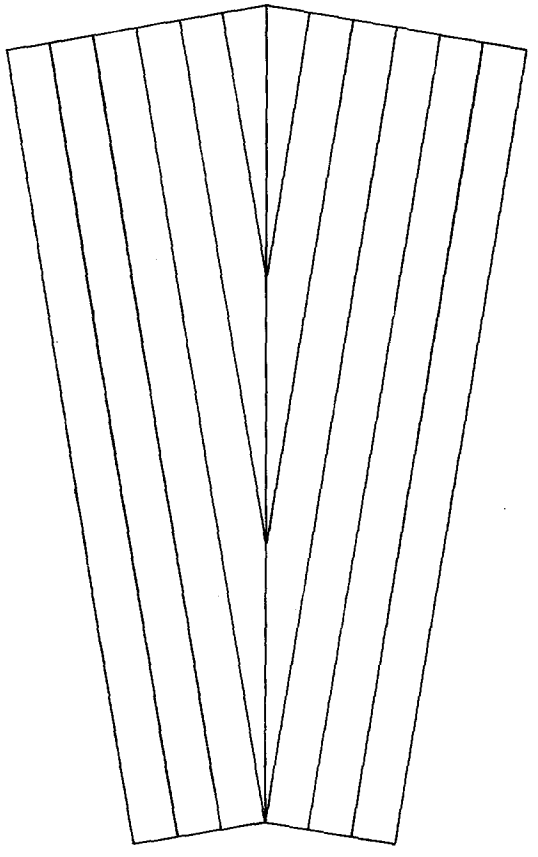

Figure 7 Stress-free grain boundary obtained when the lattice and surface dislocations are uniformly and continuously distributed within the boundary.

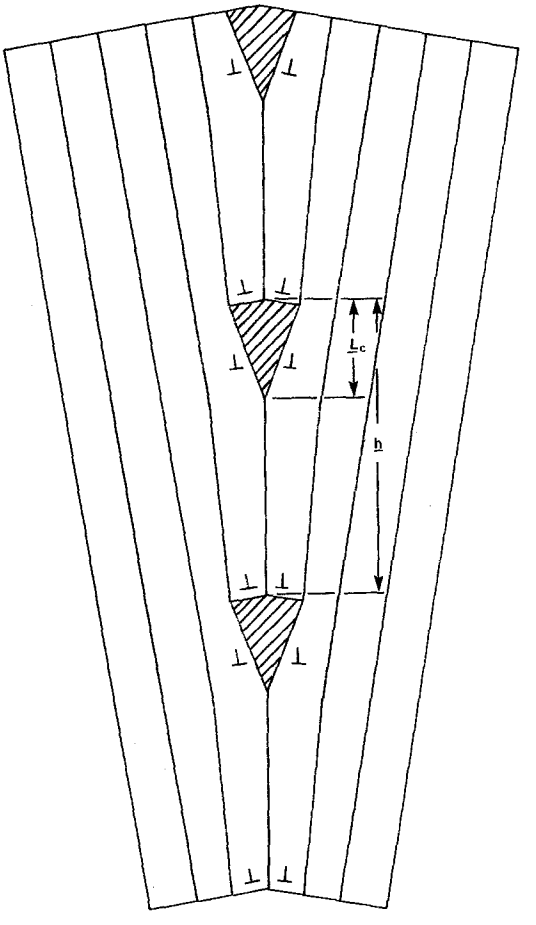

Figure 8 Grain boundary structure obtained when the dislocation configuration in Fig. 4 is allowed to dissociate by means of core formation.

result. The strength of the resulting uncompensated grain boundary dislocation $\mathbf{b}_{GB}$; i.e. that which generates a stress field, is thus simply

$$\mathbf{b}_{GB} = \mathbf{b}_L - \frac{L_c}{h}\mathbf{b}_L \tag{8}$$

or

$$\mathbf{b}_{GB} = \frac{h - L_c}{h}\mathbf{b}_L \tag{9}$$

It is clear that the reason why lattice and surface dislocations within the grain boundary can interact with one another in the way that leads to Equations 8 and 9 is due to the fact that they occupy the same surface. This is not possible for the isolated lattice dislocation of Fig. 1b which is separated from its corresponding surface dislocations by means of a doubly-connected surface.

In the limiting case where the core length L_c in Fig. 8 becomes equal to the separation h of the lattice dislocations in the boundary, $\mathbf{b}_{GB} = 0$ according to Equation 9. This simply means that all of the surface dislocations annihilate with the lattice dislocation to form stress-free edges in accordance with Equation 3. This may also be referred to as a completely torn or uncoalesced grain boundary [5]. The configuration shown in Fig. 9 can never be realized physically because it corresponds to a state of high surface energy [6, 10, 13]. However, as the angle of misorientation θ increases, h decreases in accordance with the following relationship:

$$\mathbf{b}_L = h \sin \frac{\theta}{2} \tag{10}$$

The lattice dislocation at the boundary thus loses more and more of its strength. This can be seen by referring to the 36.9° tilt boundary of Fig. 10a where the dislocation cores occupy half the area of the grain boundary. It also follows that for large angle boundaries, the dislocations comprising the

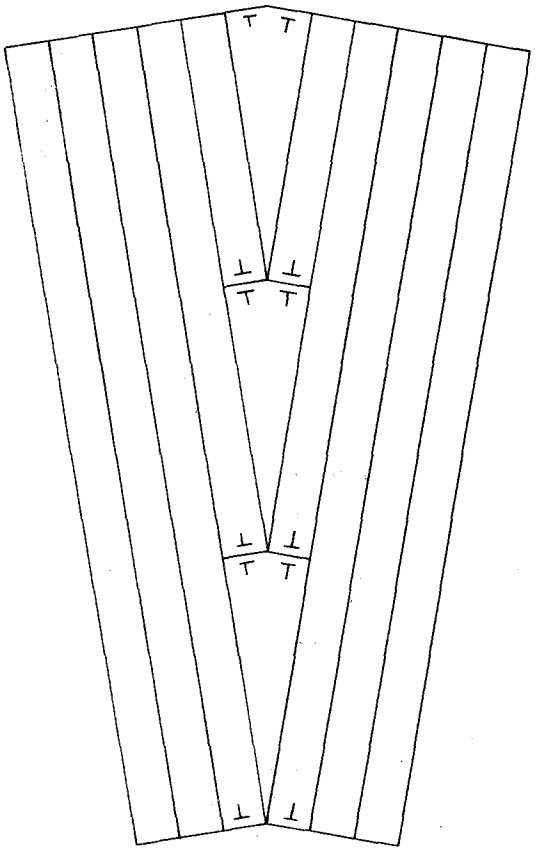

Figure 9 Limiting case of Fig. 8 where the grain boundary dislocation core length becomes equal to the dislocation separation.

boundary cannot be treated as a linear array, as in Fig. 5a. Instead, the lattice dislocation must now be distributed over the surface of the lattice dislocation core. In the limiting case when the angular misorientation between the two adjacent grains becomes equal to 90°, $L_c = h$, and we simply have the case of a perfect crystal; i.e. no grain boundary, as can be seen by reference to Fig. 10b. The fact that the strength of a grain boundary dislocation is reduced below that which it would ordinarily possess if it were situated by itself within an otherwise perfect crystal was first recognized by Jagannadham and Marcinkowski [12]. It should also be pointed out here that Equation 10 is the more exact version of Equation 1. In the former relation, each grain is treated separately, wherein the grain boundary dislocation $\mathbf{b}_L$ is associated with a particular grain. However, in Equation 1, the dislocations are assumed to be situated in one single crystal, which strictly speaking, is not possible. While it can be argued that for small values of θ the differences between Equations 1 and 10 are insignificant, it must not be forgotten that it was just this small angle approximation that for more than thirty years hampered a full understanding of the nature of grain boundaries in terms of surface dislocations.

Since the grain boundary dislocations from

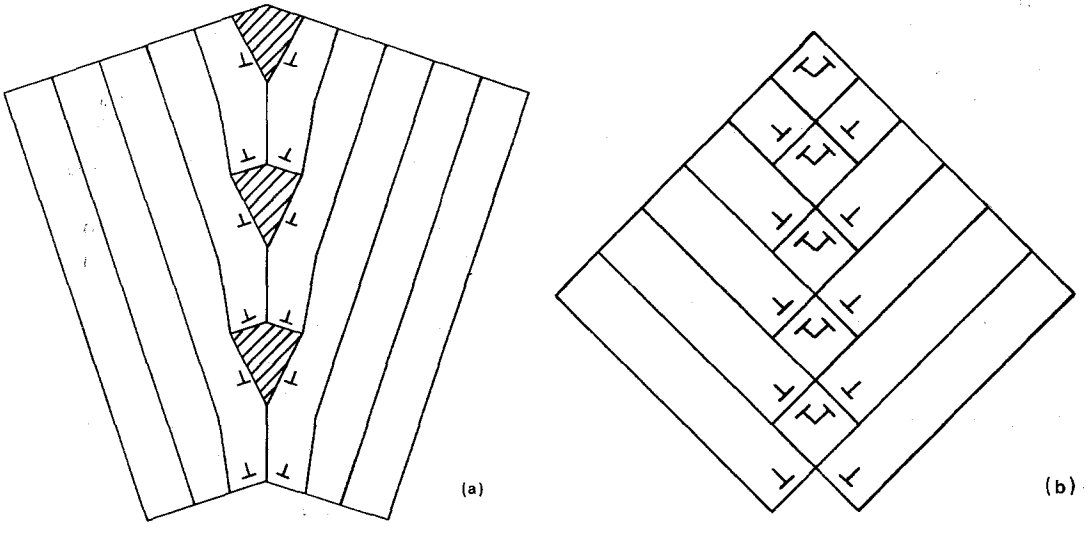

Figure 10 Symmetric tilt boundary with misorientation angle (a) 36.9°; (b) 90°.

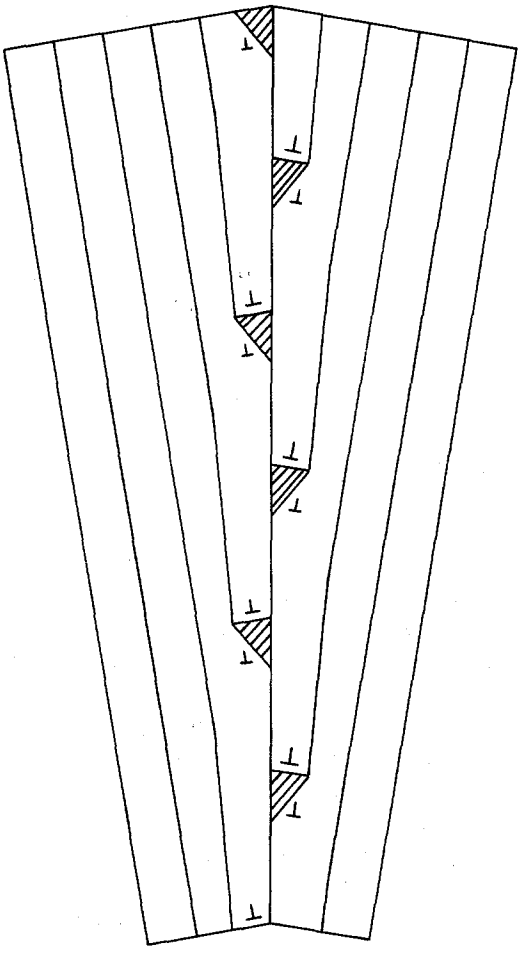

Figure 11 Reduction in energy of the grain boundary shown in Fig. 8 by dislocation climb.

each of the grains in Fig. 8 are in contact with each other at the boundary, the elastic energies are relatively high. A reduction in this energy can be attained by having them separate from one another via some mechanism such as dislocation climb into the configuration illustrated in Fig. 11, where again, for the purposes of clarity, the surface dislocation array has been omitted. Such a dissociation allows a reduction in the size of the dislocation cores and thus the elastic strain energy. Fig. 11 clearly depicts the correct model of a grain boundary for small values of θ, and is in fact the model upon which Equation 1 was predicated. Again, however, it must be emphasized that even for very low angle boundaries with configurations such as that given in Fig. 11, the surface dislocations are still present within the boundary. Furthermore, these surface dislocations lead to a finite albeit very small reduction in the strength of the lattice dislocations in accordance with Equations 8 and 9. Of further interest is the fact that the dislocation cores associated with the grain boundary dislocations of Fig. 11 are highly asymmetric as compared to the paired grain boundary dislocations of Figs. 8 and 10a or to the non-boundary dislocation of Fig. 1b.

5. Summary and conclusions

In the case of an individual crystal lattice dislocation within an otherwise perfect crystal of finite dimensions, the stress-free boundary conditions on the outer surface of the body can be satisfied by the distribution of a continuous array of infinitesimal dislocations of opposite sign to that of the lattice dislocation on the surface. The total Burger's vector of all the surface dislocations must be of the same magnitude as that of the lattice dislocation. In addition, the lattice dislocation can lower its energy by the creation of an asymmetric crack or core upon whose surface the Burger's vector of the lattice dislocation is continuously distributed. Thus, in its most general sense, a lattice dislocation in a finite body may be viewed as a doubly-connected surface upon which are distributed a continuous distribution of dislocations of opposite sign which can never come into contact with one another.

When the crystal lattice dislocations align themselves into a wall so as to form a grain boundary, then the boundary may be viewed as a surface upon which both the lattice and surface dislocations co-exist. In this special case the dislocation loses its doubly-connected surface and reverts to one of single connectivity. The classical view is to regard the grain boundary as an array of lattice dislocations only, wherein the surface dislocations are omitted. This leads to difficulties in trying to understand the structure of high angle boundaries, especially the reduced elastic strength of the dislocations comprising such boundaries. However, this difficulty is resolved with the surface dislocation approach in that, as the angle of misfit between the two grains comprising the grain boundary increases, more and more of the surface dislocations combine with the lattice dislocation to reduce its strength, while at the same time generating a stress-free ledge.

Acknowledgements

The present research was supported by the United

States Department of Energy under Contract No. DE-AS05-76ERO3935.

References

1. F. L. VOGEL, W. G. PFANN, H. E. COREY and E. E. THOMAS, *Phys. Rev.* **90** (1953) 489.
2. J. C. M. LI, "Electron Microscopy and Strength of Crystals", edited by G. Thomas and J. Washburn (Interscience Publishers, New York, 1963) p. 713.
3. S. AMELINCKX and W. DEKEYSER, "Solid State Physics" Vol. 8, edited by F. Seitz and D. Turnbull (Academic Press, New York, 1959) p. 325.
4. J. P. HIRTH and J. LOTHE, "Theory of Dislocations" (McGraw-Hill Book Company, New York, 1968).
5. M. J. MARCINKOWSKI, "Unified Theory of the Mechanical Behavior of Matter" (John Wiley and Sons, New York, 1979).
6. M. J. MARCINKOWSKI, *Phys. Status Solidi* (a) **60** (1980) 109.
7. K. JAGANNADHAM and M. J. MARCINKOWSKI, *ibid.* (a) **50** (1978) 293.
8. *Idem, ibid.* (a) **54** (1979) 715.
9. A. H. COTTRELL, "Dislocations and Plastic Flow in Crystals" (Claredon Press, London, 1953).
10. M. J. MARCINKOWSKI and K. JAGANNADHAM, *Phys. Status Solidi* (a) **50** (1978) 601.
11. K. JAGANNADHAM and M. J. MARCINKOWSKI, *Cryst. Lattice Defects* **8** (1979) 81.
12. *Idem, J. Mater. Sci.* **15** (1980) 563.
13. M. J. MARCINKOWSKI, "Dislocation Modelling of Physical Systems", edited by M. F. Ashby, R. Bullough, C. S. Hartley and J. P. Hirth (Pergamon Press, New York, 1981) p. 342.

Received 10 June
and accepted 29 July 1982